



Three-dimensional rotational spectroscopy in the submillimeter

Sarah M. Fortman, Ivan R. Medvedev, Christopher F. Neese, Frank C. De Lucia *

Department of Physics, Ohio State University, 191 W. Woodruff Ave., Columbus, OH 43210, USA

ARTICLE INFO

Article history:

Received 8 April 2010

In final form 17 May 2010

Available online 21 May 2010

ABSTRACT

There is a growing consensus that traditional approaches to submillimeter spectroscopy will continue to be outpaced by the growth of molecular astrophysics and the analytical sciences. We report here a methodology that significantly reduces this challenge by providing three-dimensions of spectroscopic information (frequency, line strength, and lower-state energy), even for complex, perturbed spectra, without the need for spectral analysis. The method is based on the analysis of complete, intensity-calibrated spectra taken over a range of temperatures. The 3D spectral information significantly reduces the assignment space and leads to much more efficient and accurate spectral assignment and quantum-mechanical modeling.

© 2010 Published by Elsevier B.V.

Rotational spectroscopy in the submillimeter (SMM) spectral region has become the foundation of numerous and diverse scientific and technical endeavors, including large astronomical instruments such as Herschel [1], ALMA [2], and SOFIA [3]; atmospheric remote sensing platforms such as MLS [4] and JEM/SMILES [5]; laboratory and chemical diagnostics [6,7]; and analytical science [8,9]. However, many of these endeavors are outpacing the laboratory spectroscopy on which they are based. This is primarily due to the extreme complexity of the spectroscopic analysis of the high-resolution rotational spectra that is the basis and strength of these fields.

Figs. 1 and 2 illustrate the spectroscopic challenge. Fig. 1 shows on a highly compressed graphical scale the spectrum of ethyl cyanide, a common astrophysical species, between 570 and 645 GHz. On an expanded graph more than 10 000 lines are clearly identifiable. Fig. 2 shows a graph of the intensity of the 9962 strongest lines, sorted according to their strength. Also shown on this graph is the intensity-sorted spectrum from current databases [10,11]. These databases contain calculated line lists based on quantum-mechanical analyses of assigned transitions in the ground vibrational state. The divergence between these two graphs occurs at the point where the Boltzmann factor of the first two excited vibrational states (ν_{21} at 222 cm^{-1} and ν_{13} at 226 cm^{-1} , which are not included in the catalogue) allow rotational transitions within the two states to make contributions to the intensity sort of the experimental data. Although analysis of these two states has begun, the complexity of the interactions and perturbations between these states makes this a challenging undertaking [12–14] and it is analyses of this type that this paper addresses. Because of the rapidly increasing density of vibrational states with energy, there are

~100 vibrational states, each with its own rotational spectrum to be assigned.

SMM spectroscopy is inherently a high-resolution discipline, with spectral widths determined by Doppler broadening on the order of 1 MHz. In order to provide the resolution required, electronic sources, often phase-locked, are combined with harmonic generation either to provide spectroscopic power from a lower frequency source [15] or to provide the frequency reference for fundamental SMM sources [16]. A traditional system might record data points at intervals of 10% of a line width, with a 1 s time constant, thus taking 10^6 s (~300 h) to record a 100 GHz spectral interval.

SMM systems are technically challenging and power variations create a complex background. An example can be seen in the intensity normalization trace included in Fig. 1, although our system, which is optimized for bandwidth, is somewhat better than typical. Power variations of a factor of five or more are common. Most detectors do not have the dynamic range required to record the DC power level and observe weak absorptions. Furthermore, the DC power level is often convolved with detector bias voltages and $1/f$ noise. In an effort to maximize sensitivity, detectors are typically AC-coupled and modulation techniques are employed that do not preserve spectral line strength information. Thus, it is technically difficult to calibrate experimental line intensities. Furthermore, it is difficult to control other factors that affect the line intensities (pressure, temperature, and baseline) over the long timescale of a traditional SMM experiment.

The large majority of spectroscopic studies in this spectral region have been carried out with an experimental–theoretical bootstrap strategy that requires only approximate intensities as an aid to assignment. The bootstrap strategy is: (1) Make an estimate of the spectrum based on previous spectral measurements and assignments. In the absence of previous assignments *ab initio* or semi-empirical molecular structure calculations are used. (2) Use

* Corresponding author.

E-mail address: fcd@mps.ohio-state.edu (F.C. De Lucia).

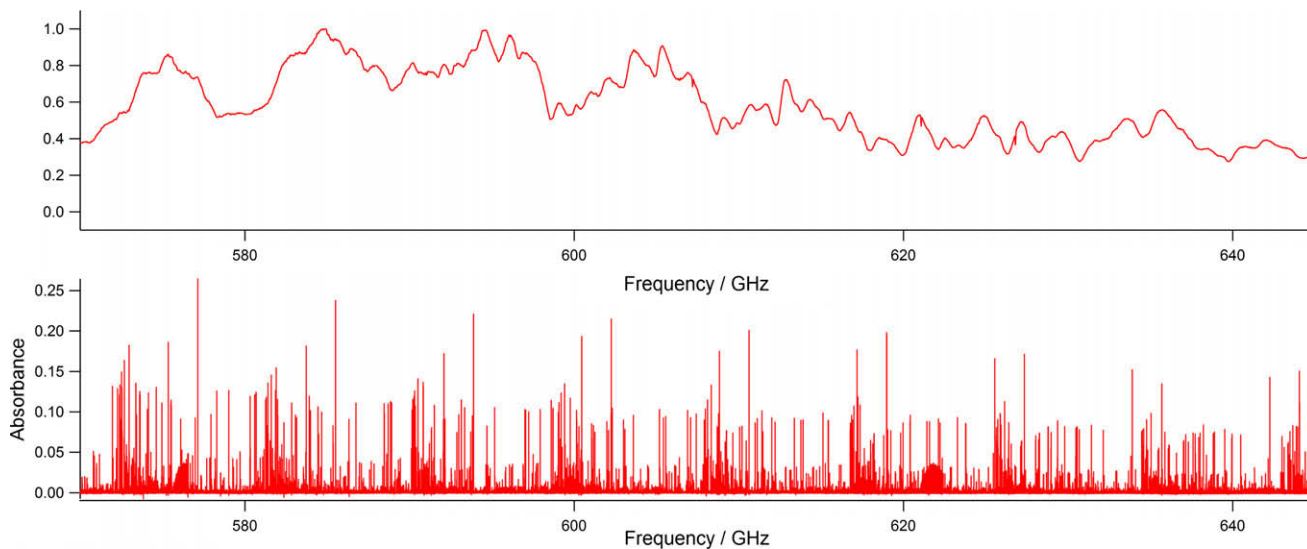


Fig. 1. The intensity-calibrated spectrum of ethyl cyanide on a highly compressed scale between 570 and 645 GHz (lower panel). The normalization factor (upper panel).

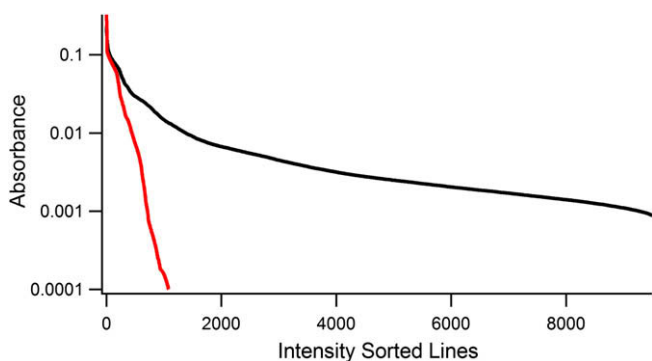


Fig. 2. The intensity of 9962 experimentally measured spectral lines, sorted according to intensity (upper black trace). The intensity of the 695 strongest predicted ground vibrational state lines, sorted according to intensity (lower red trace). The dots that represent each line are so numerous as to make them appear as lines in this figure. (For interpretation of the references to colour in this figure legend, the reader is referred to the web version of this article.)

the predicted spectrum to experimentally search for new lines to assign. (3) Use the new assignments to refine and extend the model via a least-squares fit of the line centers. Reject incorrect assignments. (4) Iterate.

For rigid molecules in unperturbed vibrational states the bootstrap process converges fairly rapidly, and is typically limited by the spectrometer's scan speed. The reason for rapid convergence is that many lines can be assigned per iteration in step (2) and the χ^2 surface minimized in step (3) is highly quadratic so that the model easily converges to highly accurate molecular constants. For 'floppy' molecules or perturbed vibrational states the process is greatly hindered. The uncertainty in the predicted line centers can become high such that per iteration there are many possible assignments, and it is only possible to assign a few lines at a time in order to avoid incorrect assignments contaminating the model. Furthermore, the model may be critically dependent on parameters that are not readily determined from the observed line centers. An example of such a parameter is the band origin of a hot band. In some cases it is possible for correctly assigned lines to degrade the predictive ability of the fit due to correlation. As a result, the analysis of spectra is very challenging and decades of work can be devoted to a single molecule.

With the traditional bootstrap approach, only a fraction of the spectral lines of a particular vibrational state are recorded and assigned; the quantum-mechanical model is used to calculate the complete rotational spectrum of the vibrational state. This approach has been successfully used to provide the spectroscopic foundation for molecules such as nitric acid [17,18] and ozone [19] for atmospheric remote sensing experiments such as MLS [4]. Unfortunately, the lack of analyses of excited vibrational states results in spectra calculated from quantum-mechanical models to be *massively incomplete*. This incompleteness has consequences for disciplines dependent on laboratory spectral information. For example, in some astronomical sources up to half of the observed lines are unidentified. Most of these lines are believed to be hot bands of a few 'weed' molecules.

It is the purpose of the work reported here to demonstrate a new approach that both addresses this massive incompleteness and significantly enhances the assignment process for quantum-mechanical models. Our approach results in a three-dimensional (frequency, line strength, and lower-state energy level) SMM line list. The traditional approach provides a one-dimensional (frequency) line list, since intensity is normally uncalibrated and seldom published. Briefly, we will show how it is possible to first obtain accurate spectroscopic intensities in the SMM and then use these intensities, obtained for spectra taken over a range of temperatures, to obtain accurate lower-state energy levels and line strengths. This three-dimensional database can significantly aid the bootstrap assignment process by limiting the number of possible assignments in step (2). Furthermore, the lower-state energies can provide spectroscopic information missing from the line centers, aiding step (3). Although not the focus of this paper, this approach is also capable of producing 'complete' spectral maps as a function of temperature without the need for the aforementioned bootstrap assignment process [20,21]. These complete, temperature calibrated spectra provide a means to attack problems such as the astrophysical 'weeds'.

We have previously reported an alternative to the traditional phase lock, FM modulation [15,22,23] approach to SMM spectroscopy, FAST Scan Submillimeter Spectroscopic Technique (FASST). The FASST spectrometer provides some of the elements required for the work reported here [24,25]. In this approach, the SMM frequency is scanned rapidly enough ($\sim 1\text{--}10$ GHz/s) such that the Fourier components that contain the absorption line information are at frequencies high enough to be above the $1/f$ noise of the sys-

tem. With appropriate bandwidth in the detector channel, it is then possible to record near true line shape spectra directly and very rapidly. Speed is essential for the work reported here because it requires temperature and number density stability over the period required to record a complete spectrum.

For this work we used a solid-state implementation of the earlier Backward Wave Oscillator (BWO) based FASSST. In this system, an Agilent E8256D synthesizer is used to generate power between 11.875 and 13.45 GHz. This power is subsequently multiplied by a Virginia Diodes, Inc. $\times 48$ multiplier chain, transmitted through the experimental cell and detected by an InSb hot electron bolometer. The cell consists of a 15 cm diameter aluminum tube, cooled convectively by liquid nitrogen cooled fins inside a thermally insulated box, and heated electrically at ten locations to provide a uniform ramp temperature. As measured by ten thermocouples distributed along the length of the cell, the largest temperature variation was 3 K, near the window regions at the ends. In operation, the system was first cooled with liquid nitrogen and then ramped with electric heaters from 247 to 392 K over a period of several hours. In order to preserve sample purity, the sample was slowly flowed through the cell. Since each of the spectral runs required only ~ 40 s, it was possible to record spectra at 271 temperatures with a temperature variation of ± 0.5 K.

As is typical of SMM systems, the low frequency portion of the signal channel (which contains the DC power level) is not retained, both to reject the aforementioned $1/f$ noise and to increase the sensitivity of the system. In this particular case, the system was swept at ~ 2 GHz/s, which when combined with the ~ 1 MHz Doppler width in this frequency range placed the fundamental Fourier component at ~ 2 kHz, with it and the higher frequency components within the passband of the signal channel.

To remove the baseline from spectra, a peak finder was used to locate and remove the lines, and a spline fit was used to fill in the gaps. This baseline was then subtracted from the observed spectra. The absolute power level was obtained by chopping the source at ~ 2 kHz and recording this power level. In order to produce the absolute intensity-calibrated spectra, the 271 baseline subtracted spectra were then divided by the absolute intensities obtained with the chopper. We will show below that this procedure produced intensity calibration of 1%.

In addition to the need for intensity-calibrated spectra, our approach requires at least one assigned line as a reference. In practice it is useful to have many to provide redundancy, allow for the spectroscopic determination of temperature, guard against systematic effects, and assess accuracy. For this work we chose 163 relatively strong a-type transitions that were free of blends and which corresponded to assigned ground state lines. At each of the 271 temperatures, we performed a least-squares fit of the peak absorbances A_{peak} of these lines to [22,26]

$$A_{\text{peak}} = \frac{nL}{Q} \frac{8\pi^3}{3ch} (1 - e^{-h\nu_0/kT}) S_{ij} \mu^2 e^{-E_i/kT} \sqrt{\frac{\ln(2)}{\pi}} \frac{\nu_0}{\delta\nu_D} \quad (1)$$

where n is the number density of the sample, L the length of the cell, ν_0 the line frequency, $\delta\nu_D$ the Doppler width (which is a known function of temperature and frequency), T the temperature, Q the partition function, $S_{ij}\mu^2$ the line strength (including degeneracy [22]), and E_i the lower-state energy. The free parameters of this fit were nL/Q and T , allowing the concentration in the cell to vary between temperature scans (but not within an individual scan) without adversely affecting the results. Because T is a fitting parameter and because we invert Eq. (1) to calculate the line strength and lower-state energy, variations in T that occur either because of the effect of the temperature ramp over the time of the spectral sweep or because of temperature variations in the cell, do not impact the results. This is true as long as the changes in temperature are small en-

ough that a linear average of the contributions from each of the temperature regions is a good approximation. To check this approximation, we sorted the 163 fits according to lower-state energy to look for systematic effects, which were not observed. Moreover, even if there had been systematic effects, they were included in the 1% error of the temperature fits.

The fractional rms deviation of the least-squares fit is 1%, attesting to the accuracy of the intensity calibration and the constancy of nL/Q within a given temperature scan. We also validate that we are operating in a linear response region of the system by sorting the residuals according to line intensity. With proper calibration of the experimental intensity, we observe no systematic effect.

However, the b-type transitions, which were not used as reference lines, were systematically weaker relative to the quantum-mechanical predictions by 13%. This is a surprising result because for relatively rigid molecules, such as ethyl cyanide, intensities based on Stark Effect measurements [27] are ordinarily considered to be very accurate. In addition to the Stark measurements used in the catalogues there is an earlier Stark measurement [28], but it predicts a ratio that is 15% too large. Since both of these results are far outside the scatter of our intensity measurements, we have adopted the catalogue value of $\mu_a = 3.85$ D and, to yield a ratio in agreement with our intensity based experimental ratio, adjusted μ_b to be 1.31 D.

To obtain the lower-state energy and line strength for unassigned lines, the temperature measurement process of Eq. (1) can be inverted, with the lower-state energy E_i and the transition strength $S_{ij}\mu^2$ as the free variables. While in principle, spectra at only two temperatures are required for this calculation, data from all 271 temperature runs were included in the fit.

A log plot in $1/kT$ yields a straight line, with the intercept providing the line strength and the slope the lower-state energy for the unassigned line.

The accuracy of the lower-state energies can be evaluated by inspection of the 585 assigned lines that are among the 3355 strongest. Inspection of the difference between the experimental value and the results of the quantum-mechanical calculation for the 93 lines whose absorbances are above 0.1 shows an rms scatter of ~ 15 cm^{-1} . For the full set of 585 lines there are a few large outliers that have deviations of 100–1000 cm^{-1} , presumably due to overlaps with unassigned lines. From this we conclude that the errors in the experimentally determined lower-state energies for unblended lines are 10–20 cm^{-1} , with some increase in uncertainty for weaker lines. The larger differences occur because the incompleteness of the quantum-mechanical model results in predictions that do not include all the spectral intensity at the positions of each catalogued line.

Fig. 3 shows the three-dimensional line list of ethyl cyanide on a highly compressed scale. However, even on this scale it is possible to observe a number of important features. The most prominent features are the strong ground vibrational state a-type R-branches that are along the solid line and which have branches that diverge rapidly to higher energy each ~ 10 GHz. In addition, there are two strong b-type Q-branch features of roughly constant frequency, one near 575 GHz and the other near 620 GHz. Additional b-type transitions lie along and are scattered above the double dot dashed line.

The next most prominent patterns in the experimental spectrum, which lie along the dotted line, are the a-type transitions of the two lowest vibrational states, ν_{21} at 222 cm^{-1} and ν_{13} at 226 cm^{-1} . It is these lines, which are not included in the quantum-mechanical catalogue, that cause the divergence between the experimental and catalogue intensity distribution shown in Fig. 2. Additionally, the next lowest vibrational state is ν_{20} which lies at 378 cm^{-1} . The dashed line highlights the a-type R-branches for this state along with those for the $2\nu_{13}$, $2\nu_{21}$, and $\nu_{13} + \nu_{21}$. It is

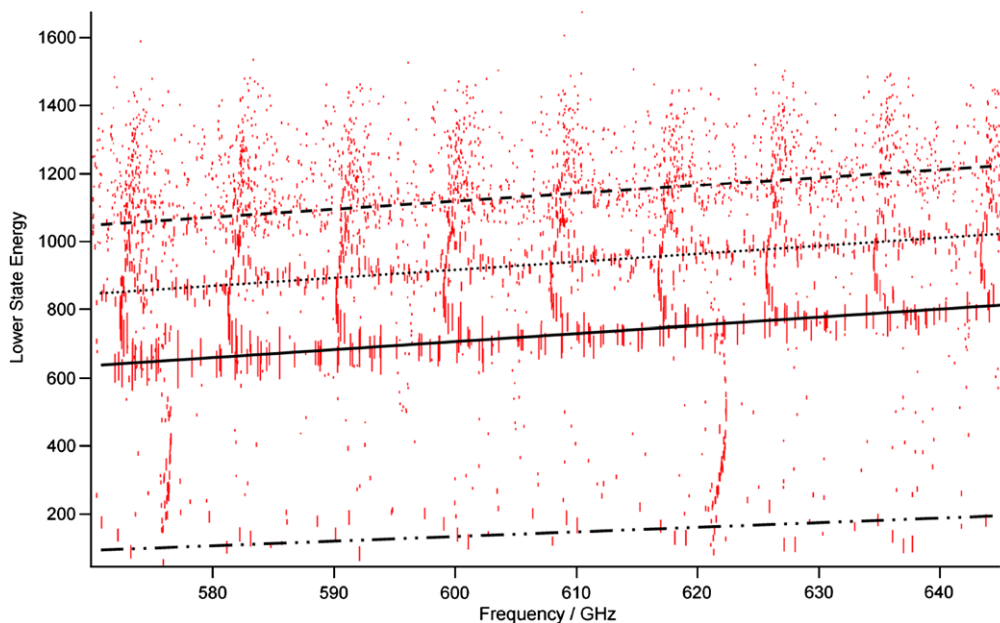


Fig. 3. The three dimensional spectrum of ethyl cyanide on a highly compressed scale, with the length of the line being the pseudo third dimension representing line strength (indicated by the length of the line), with the location of the base of the line indicating the lower-state energy. In order to reduce overlap and facilitate the recognition of the spectra according to vibrational state, the intensity scale is substantially foreshortened.

this rapid growth of vibrational state density that accounts for the density of observed lines in the intensity-calibrated spectrum, as illustrated in Figs. 1 and 2. While there is limited visibility of the intensity axis in this projection of the 3D image, for step 2 of the bootstrap assignment process discussed above, all of these identifications are much easier with the numerical data rather than the graphical realization in Fig. 3.

The complexity of rotationally resolved spectra has motivated many to consider automated [29,30] or semi-automated approaches [31]. However, the multiplicity of assignment choices, constrained only by the accuracy of the theoretical frequency prediction and an approximate experimental intensity, can be very large. Since our lower-state energies are constrained within 1–5% of the range of possibilities, these data will constrain assignment choices and should make possible new approaches for automated spectral assignment.

Three-dimensional rotational spectroscopy in the SMM is a significant advance both for fundamental spectroscopic analyses and for applications built upon SMM rotational spectroscopy. It provides:

1. Direct experimental measurement of not only line frequencies, but also of transition strengths and lower-state energies. With current approaches, these are only obtained at the end of iterative bootstrap spectral analyses.
2. A means for obtaining correct transition strengths for each transition even for molecules whose distortions, internal motions, etc. introduce uncertainty into the quantum-mechanical calculation. It also provides a check on the dipole moment transition moments calculated from Stark effect measurements.
3. A direct measure of the partition function. In molecules with low-lying vibrational and torsional states, the calculation of this quantity is often not straightforward.

Acknowledgements

We would like to thank the National Science Foundation and JPL/Herschel for their support of this work. This work was also sup-

ported by NASA Headquarters under the NASA Earth and Space Science Fellowship Program – Grant NNX09AP10H.

References

- [1] D. Clery, *Science* 324 (2009) 584.
- [2] J.L. Turner, H.A. Wooten, *Highlights Astronomy* 14 (2006) 521.
- [3] E.E. Becklin, *Adv. Space Res.* 36 (2005) 1087.
- [4] J.W. Waters et al., *J. Atmos. Sci.* 56 (1999) 194.
- [5] J. Inatani et al., *Proc. SPIE* 4152 (2000) 243.
- [6] D.D. Skatrud, F.C. De Lucia, *Appl. Phys. Lett.* 46 (1985) 631.
- [7] H.O. Everitt, F.C. De Lucia, in: B. Benderson, H. Walther (Eds.), *Advances in Atomic and Molecular Physics*, Academic, San Diego, 1995, pp. 331–400.
- [8] S. Albert, D.T. Petkie, R.P.A. Bettens, S. Belov, F.C. De Lucia, *Anal. Chem.* 70 (1998) 719A.
- [9] I. Medvedev, M. Behnke, F.C. De Lucia, *Analyst* 131 (2006) 1299.
- [10] H.M. Pickett, R.L. Poynter, E.A. Cohen, M.L. Delitsky, J.C. Pearson, H.S.P. Muller, *J. Quant. Spectrosc. Radiat. Transfer* 60 (1998) 883.
- [11] H.S.P. Müller, F. Schlöder, J. Stutzki, G. Winnewisser, *J. Mol. Struct.* 742 (2005) 215.
- [12] Y. Fukuyama, K. Omori, H. Odashima, K. Takagi, S. Tsunekawa, *J. Mol. Spectrosc.* 193 (1999) 72.
- [13] C.S. Brauer, J.C. Pearson, B.J. Drouin, S. Yu, 64th OSU International Symp. Mol. Spectrosc., Columbus, 2009.
- [14] C.S. Brauer, J.C. Pearson, B.J. Drouin, S. Yu, *ApJ Suppl. Ser.* 184 (2009) 133.
- [15] P. Helminger, F.C. De Lucia, W. Gordy, *Phys. Rev. Lett.* 25 (1970) 1397.
- [16] A.F. Krupnov, A.V. Burenin, in: K.N. Rao (Ed.), *Molecular Spectroscopy: Modern Research*, Academic Press, New York, 1976, pp. 93–126.
- [17] G. Cazzoli, F.C. De Lucia, *J. Mol. Spectrosc.* 76 (1979) 131.
- [18] D.T. Petkie, T.M. Goyette, P. Helminger, H.M. Pickett, F.C. De Lucia, *J. Mol. Spectrosc.* 208 (2001) 121.
- [19] H.M. Pickett et al., *J. Mol. Spectrosc.* 128 (1988) 151.
- [20] I.R. Medvedev, F.C. De Lucia, *ApJ* 656 (2007) 621.
- [21] S.M. Fortman, I.R. Medvedev, C.F. Neese, F.C. De Lucia, *ApJ* 714 (2010) 476.
- [22] C.H. Townes, A.L. Schawlow, *Microwave Spectroscopy*, McGraw-Hill Dover Publications, Inc., New York, 1955.
- [23] P. Helminger, J.K. Messer, F.C. De Lucia, *Appl. Phys. Lett.* 42 (1983) 309.
- [24] D.T. Petkie, T.M. Goyette, R.P.A. Bettens, S. Belov, S. Albert, P. Helminger, F.C. De Lucia, *Rev. Scient. Instrum.* 68 (1997) 1675.
- [25] I. Medvedev, M. Winnewisser, F.C. De Lucia, E. Herbst, E. Białkowska-Jaworska, L. Psczolkowski, Z. Kisiel, *J. Mol. Spectrosc.* 228 (2004) 314.
- [26] W. Gordy, R.L. Cook, *Microwave Molecular Spectra*, John Wiley & Sons, New York, 1984.
- [27] H.M. Heise, H. Lutz, H. Dreizler, *Z. Naturforsch.* 29a (1974) 1345.
- [28] V.W. Laurie, *J. Chem. Phys.* 31 (1959) 1500.
- [29] G. Moruzzi, *J. Mol. Spectrosc.* 229 (2005) 19.
- [30] W.L. Meerts, *Phys. Scripta* 73 (2006) C47.
- [31] I. Medvedev, M. Winnewisser, B.P. Winnewisser, F.C. De Lucia, E. Herbst, *J. Mol. Struct.* 742 (2005) 229.